Published online April 3, 2006

Transport of *Giardia* and Manure Suspensions in Saturated Porous Media

Scott A. Bradford,* Yadata F. Tadassa, and Yakov Pachepsky

ABSTRACT

Experiments were conducted to elucidate the transport behavior of cysts of *Giardia* and manure suspensions through several aquifer sands. Decreasing the median grain size of the sand resulted in lower peak effluent concentrations and increased deposition of the *Giardia* and manure particles in the sand near the column inlet. The effluent concentration curves for the manure suspensions also exhibited asymmetric shapes that tended to include larger particle sizes as the manure suspension was continuously added. Simulations of the transport of *Giardia* and manure particles using a simple and flexible power law model for the solid-water mass exchange term provided a satisfactory description of the effluent and spatial distribution data. The cumulative size distribution (CSD) of manure particles in the suspension initially and after passage through the packed columns was used to identify the mechanisms that were controlling the deposition of manure particles and *Giardia*. The CSD data indicated that manure particles were completely removed at early times by mechanical filtration and/or straining when the ratio of the particle to the median grain diameter was greater than 0.003 to 0.017. However, the CSD changed with increasing time due to deposition-induced filling of straining sites. The *Giardia* transport was controlled by straining. For a given sand, higher effluent concentrations of *Giardia* were observed in the presence than in the absence of manure suspension. The relative increase of *Giardia* in the effluent concentrations varied from 75 to 172%. Hence, pathogen transport studies conducted in the absence of manure suspension may underestimate transport potential in manure-contaminated environments.

Concentrated animal feeding operations (CAFOs) produce large quantities of manure, wash water, and storm water runoff. More than 272 million tonnes of manure were produced by confined beef and dairy cows (*Bos taurus*) in the USA in 1997 (Kellogg et al., 2000). These wastes can pose a risk to human health due to the presence of a variety of pathogenic microorganisms (Gerba et al., 1996; Loge et al., 2002). Cysts of *Giardia*, one type of pathogenic protozoan parasite, are commonly found in human and animal wastes (Hoogenboezem et al., 2001). When cysts are ingested they can cause a gastrointestinal disease called giardiasis that produces diarrhea, fatigue, and abdominal/stomach cramps in infected humans. The USEPA requires water utilities using surface water or ground water under the influence of surface water as a source of drinking water to remove 99.9% of the *Giardia*, and has established a maximum contaminant level goal of zero cysts (USEPA, 2000).

S.A. Bradford and Y.F. Tadassa, USDA–ARS, George E. Brown Jr. Salinity Lab., 450 W. Big Springs Rd., Riverside, CA 92507-4617; Y. Pachepsky, USDA–ARS, Environmental Microbial Safety Lab., Bldg. 173, Rm. 203, BARC–East Power Mill Rd., Beltsville, MD 20705. Received 7 June 2005. *Corresponding author (sbradford@ussl.ars.usda.gov).

Published in J. Environ. Qual. 35:749–757 (2006).
Technical Reports: Ground Water Quality
doi:10.2134/jeq2005.0226

677 S. Segoe Rd., Madison, WI 53711 USA

Hancock et al. (1998) indicated that *Giardia* were sometimes present in ground water, especially in infiltration galleries and horizontal wells. Consistent with this finding, 6% of the ground water–associated disease outbreaks in the USA from 1971 to 1996 have been attributed to *Giardia* (USEPA, 2000). This information has important implications for treatment techniques of surface water or effluent from sewage treatment plants that rely on soil passage to remove cysts (i.e., riverbank filtration, infiltration basins and trenches, and sand filters). It also implies that ground water under the direct influence of surface water may be vulnerable to contamination by *Giardia*. Hence, knowledge of the processes and factors that control the transport and deposition of cysts in soils is needed to protect drinking water supplies.

Considerable research has been devoted to the transport and fate of bacteria and viruses in porous media (reviews are given by Schijven and Hassanizadeh, 2000; Harvey and Harms, 2002; Jin and Flury, 2002; Ginn et al., 2002; de Jonge et al., 2004). Cysts of *Giardia* are much larger (8–12 μm) than most of these waterborne pathogens (<2 μm). Because of their relatively large size, *Giardia* are typically assumed to have limited transport potential and little research has therefore examined their transport in porous media (Swertfeger et al., 1999; Hsu et al., 2001). Several studies have, however, examined the transport and deposition behavior of *Cryptosporidium* oocysts (Mawdsley et al., 1996a, 1996b; Brush et al., 1999; Swertfeger et al., 1999; Harter et al., 2000; Hsu et al., 2001; Logan et al., 2001; Tufenkji et al., 2004; Bradford and Bettahar, 2005; Tufenkji and Elimelech, 2005). *Cryptosporidium parvum* is also a pathogenic protozoan parasite, but is smaller in size (3–6 μm) than *Giardia*. Results from these studies suggests that deposition of *Cryptosporidium* oocysts in porous media will depend on a specific combination of physical (grain size and surface roughness, pore water velocity, and preferential flow pathways) and chemical (oocyst chemical properties, grain surface charge, and solution pH and ionic strength) properties of a given system.

Attachment, mechanical filtration, and straining are potential mechanisms for colloid (cysts of *Giardia*) deposition that have been identified (McDowell-Boyer et al., 1986). Attachment involves collision with and fixation to the porous medium, and depends on colloid–colloid, colloid–solvent, and colloid–porous media interactions (Elimelech and O'Melia, 1990). Clean-bed attachment behavior is traditionally described as a first-order process and the spatial distribution of retained colloids will hence assume an exponential shape (e.g.,

Abbreviations: CAFO, concentrated animal feeding operation; CSD, cumulative size distribution; DOM, dissolved organic matter; EC, electrical conductivity; MSE, mean square error; PV, pore volume.

Tufenkji et al., 2003). Mechanical filtration refers to the complete retention of colloids at the soil surface because the colloids are larger than the soil pores (McDowell-Boyer et al., 1986). Straining involves the entrapment of colloids in down-gradient pores and at grain junctions that are too small to allow particle passage, and consequently increases with increasing size of the colloid and decreasing sand size (Bradford et al., 2003). In contrast to mechanical filtration, straining only happens in the smaller portions of the pore space and transport of colloids can still occur in the pore networks that are larger than the colloid diameter. Straining is most pronounced at the soil surface or at the boundary of different soil textures where colloids are encountering a new pore network (Bradford et al., 2002, 2003, 2004, 2005). At such boundaries, colloids are more likely to encounter a pore smaller than the critical straining size or a pore larger than the critical size that steers colloids toward "dead-end regions" of the pore space. Once colloids have entered the hydraulically active network, size exclusion and advection make it more likely for the colloids to be transported within the network because it is formed by relatively large pores. Water permeability functions of sandy soils (e.g., van Genuchten et al., 1991) show that most of the saturated flow in sands occurs in large pores that are substantially larger than colloid sizes.

Although pathogens are of fecal origin, most transport experiments have been conducted in the absence of dissolved manure suspensions. Manure suspensions consist of a complex mixture of partially digested organic matter and microbial biomass, and therefore encompasses a wide range in particle sizes. Pathogens constitute only a small portion of the colloid-sized particles in this suspension. The subsurface transport of pathogens such as *Giardia* are likely to be influenced by the presence of this complex mixture. For example, straining and/or mechanical filtration of larger manure particles could decrease the effective size of the pores or fill and/or block smaller pore spaces completely. The potential implications of such manure deposition on pathogen transport are not yet known, and no published studies have examined the transport behavior of manure suspensions in conjunction with pathogen transport. Manure deposition induced changes in the soil pore sizes could also promote pathogen retention via straining, or induce changes in the pore-scale water flow field that would confine pathogens to more conductive (larger and less reactive) regions of the pore space.

Published research using dissolved organic matter (DOM) such as humic and fulvic acids suggests that manure suspensions may also influence the attachment behavior of pathogens. For example, DOM has been reported to enhanced microbe transport (Johnson and Logan, 1996; Pieper et al., 1997; Powelson and Mills, 2001). Blocking of favorable attachment sites by organic matter has typically been used to explain this enhanced transport (Johnson and Logan, 1996; Pieper et al., 1997). Dissolved organic matter has also been reported to sorb onto bacterial cell walls and alter their electrophoretic mobility (Gerritson and Bradley, 1987). Increasing the negative charge of the bacterial surface diminishes its attachment onto negatively charged solid surfaces (Sharma et al., 1985). Other researchers have reported that organic matter inhibits microbe transport due to hydrophobic interactions between microbe and grain surfaces that are coated with organic matter (Bales et al., 1993; Kinoshita et al., 1993). Adsorption of pathogens onto mobile manure colloids could also facilitate their transport potential (Jin et al., 2000; de Jonge et al., 2004).

This study examines the transport of manure suspensions and cysts of *Giardia* in several sands. Special attention was given to mechanisms of manure particle and *Giardia* deposition, and the influence of manure suspensions on cyst migration. Effluent concentration curves, deposition data, temporal changes in the manure effluent size distribution, and numerical modeling were used to quantify mechanisms controlling the transport and deposition of manure particles and *Giardia* in several sands. To help identify the role of manure suspension on *Giardia* transport, migration behavior in the presence and absence of manure suspensions was compared.

MATERIALS AND METHODS

Aqueous Solutions

Experimental solutions consisted of 0.001 *M* NaBr (influent suspension) or 0.001 *M* NaCl (resident and eluant solution) buffered to a pH of approximately 6.7 using 5×10^{-5} *M* $NaHCO_3$. The electrical conductivity (EC) of these solutions was 0.14 dS m^{-1}.

Manure Suspension

Dairy calf manure was collected under the crates of 1- to 12-wk-old calves, thoroughly mixed with a stick, and then stored at 4°C. The manure suspension was prepared by mixing a known mass of this manure (wet wt.) with the 0.001 *M* NaBr solution. This suspension was then filtered through a 103-μm stainless steel wire mesh. The concentrated suspension was then diluted to achieve a concentration of approximately 4.0 g L^{-1} (mass based on unfiltered weight). The pH and EC of the filtered manure suspension were 8.8 and 0.38 dS m^{-1}, respectively. The optical density at 660 nm was measured on liquid samples containing manure suspension using an Unico UV-2000 spectrophotometer (United Products & Instruments, Dayton, NJ). The manure suspension concentration was determined from a linear calibration curve between standard manure suspensions and optical density readings. Particle-size distribution information for selected liquid samples containing manure suspension were determined using a Horiba LA 930 laser scattering particle size analyzer (Horiba Instruments, Irvine, CA).

Cysts of Giardia

Cysts of *Giardia* range in size from 8 to 12 μm in diameter, and their density is around 1.04 g cm^{-3} (Medema et al., 1998). The electrophoretic mobility of the *Giardia lamblia* cysts obtained from Waterborne (New Orleans, LA) was measured to be -0.88 μm s^{-1} V^{-1} cm (corresponding to a zeta potential of -12 mV) in the 0.001 *M* NaBr solution using a ZetaPALs instrument (Brookhaven Instruments Corp., Holtsville, NY).

The concentrations of *Giardia* in liquid samples were determined using the protocol described by Bradford and Schijven (2002). In brief, 0.5 mL of concentrated (10×) PST solution was added to 4 mL of the aqueous sample to facilitate the release of cysts and to minimize sorption losses. The PST (1×) solution consists of phosphate buffered saline solution containing 2% (mass/volume) sodium dodecyl sulfate, and 2% (v/v) Tween 80. This solution was gently mixed and then centrifuged for 10 min at 1150 × *g*. The supernatant was pipetted down to 300 μL and the pellet was resuspended. Cysts were subsequently stained with 100 μL of Aqua-Glo FITC monoclonal antibody (Waterborne, New Orleans, LA) and incubated in the dark for 30 to 45 min at 37°C. After staining, the suspension was washed with 2 mL of (1×) PST, centrifuged, pipetted down to approximately 100 μL, and the pellet was resuspended. Final volumes of the stained suspension were determined by weight. A 10-μL aliquot of the suspension was then placed in a microscope well, air-dried using a hot air gun, and fixed to the slide well using 10 μL of DAPCO/glycerol mounting medium. A cover slip was placed on the slide and *Giardia* counts were made at 150× magnification using an epifluorescent microscope. The concentration was determined from the count, well volume, stained suspension volume, and initial volume of the aqueous sample.

Naturally occurring cysts of *Giardia* in the manure were used in the experiments in the presence of manure suspension. The concentration of cysts of *Giardia* in the 4 g L^{-1} manure suspension was determined to be 2.11 × 10^6 N_c L^{-1} (N_c denotes the number of cysts) using the enumeration protocol discussed above. Experiments conducted in the absence of manure suspension employed live *Giardia lamblia* cysts that were obtained from Waterborne (New Orleans, LA). The influent concentration of cysts of *Giardia* in these experiments was determined to be 8.23 × 10^6 N_c L^{-1}.

Porous Media

Ottawa aquifer sand (U.S. Silica, Ottawa, IL) was used in the transport experiments. The Ottawa sands will be designated herein by the median grain size (d_{50}) as follows: 710, 360, 240, and 150 μm. The coefficient of uniformity ($U_i = d_{60}/d_{10}$; here *x*% of the mass was finer than d_x) of the 710-, 360-, 240-, and 150-μm sands was 1.21, 1.88, 3.06, and 2.25, respectively. Ottawa sands typically consisted of 99.8% SiO_2 (quartz) and trace amounts of metal oxides, were spheroidal in shape, and had rough surfaces. The vast majority of the sands possessed a net negative charge at a neutral pH. Pore-size distribution information for these Ottawa sands can be calculated from the capillary pressure–saturation curve presented by Bradford and Abriola (2001).

Herzig et al. (1970) calculated the volume of spherical colloids that could be retained in pores based on geometric considerations. The percentage of the total column volume retained by straining was calculated (assuming a porosity of 0.35, a cyst diameter of 10 μm, a grain diameter equal to d_{10}, and the number of contact points between grains to be 7) to be 0.04% for the 710 μm sands, 0.51% for the 360 μm sands, 3.28% for the 240 μm sands, and 5.76% for the 150 μm sands. Although these straining volumes are quite small, significant numbers of cysts are required to fill these sites (Foppen et al., 2005). For example, 2.0 × 10^{10} cysts (10 μm) would be required to fully saturate (fill) all the straining sites in uniform 150-μm sand packed in a column that is 10 cm long and has an inside diameter of 5 cm. This corresponds to complete retention of cysts of *Giardia* in 38 142 pore volumes (PV) of suspension at a concentration of 8.23 × 10^6 N_c L^{-1}.

Column Experiments

Many of the experimental protocols were described in detail by Bradford et al. (2002), only an abbreviated discussion is given below. Borosilicate glass chromatography columns (15 cm long and 4.8 cm i.d.) equipped with a standard flangeless end fitting at the column bottom and a flow adaptor at the top were used in the transport studies. The columns were wet packed with the various porous media, with the water level kept a few centimeters above the soil surface. Table 1 provides porosity (ε) values determined according to the method of Danielson and Sutherland (1986) and column lengths for each experimental soil column. A multi-head drive pump was used to pump the tracer suspension (with and without manure suspension) or eluant (0.001 *M* NaCl) upward through the vertically oriented columns at a steady-rate. Effluent samples were collected in glass test tubes using an autosampler over the course of each experiment, and concentrations of *Giardia* and manure suspension were measured using the analytical procedures outlined above. The duration of the tracer suspension pulse and the average aqueous Darcy velocity (*q*) for the various column experiments is given in Table 1.

Following completion of the transport experiments, the spatial distribution of *Giardia* and/or manure suspension in the column was determined. The saturated porous medium was carefully excavated into 50-mL Falcon tubes containing excess 0.001 *M* NaBr solution, and then shaken for 15 min. The concentration of *Giardia* and/or manure suspension in the excess 0.001 *M* NaBr solution was then measured using the previously discussed analytical procedures. Liquid and sand-filled tubes were placed in an oven (100°C) overnight to volatilize the remaining solution from the sand. The volume of solution and mass of sand in each tube was determined from mass balance.

A number balance was conducted at the end of each experiment using the *Giardia* and/or manure suspension effluent and deposition data. The calculated number in the effluent and

Table 1. Soil column properties (manure suspension concentration, C_{im}; suspension pulse duration, T_o; Darcy water velocity, *q*; porosity, ε; and column length, L_c) and the percentage recovery in the effluent (F_{eff}), sand (F_{sand}), and the total system (F_{total}). The difference in F_{eff} (ΔF_{eff}) for *Giardia* in the presence and absence of the manure suspension is also provided.

Colloid	Sand	C_{im}	T_o	q	ε	L_c	F_{eff}	F_{sand}	F_{total}	ΔF_{eff}
	μm	g L^{-1}	min	cm min^{-1}		cm				
Manure	710	4	300	0.10	0.37	13.2	69.8	52.0	121.8	
Manure	360	4	300	0.10	0.32	12.2	45.1	64.4	109.5	
Manure	240	4	300	0.10	0.32	12.2	27.1	78.7	105.8	
Manure	150	4	300	0.10	0.32	12.3	21.2	83.0	104.2	
Giardia	710	0	75	0.12	0.34	12.6	1.8	94.7	96.5	
Giardia	360	0	75	0.10	0.33	12.4	0.4	77.9	78.3	
Giardia	150	0	75	0.11	0.35	12.8	0.0	65.5	65.5	
Giardia	710	4	500	0.09	0.37	13.2	4.9	62.3	67.2	3.1
Giardia	360	4	500	0.09	0.33	12.4	0.7	50.1	50.8	0.3
Giardia	150	4	500	0.10	0.35	12.9	0.6	35.9	36.5	0.6

sand was normalized by the total amount injected into a column. Table 1 presents the calculated percentage recovery in the effluent (F_{eff}), sand (F_{sand}), and the total system (F_{total}) for the various experimental systems.

Modeling

The HYDRUS-1D computer code (Simunek et al., 1998) was used to simulate the manure suspension and *Giardia* transport and deposition in the column experiments. Bradford et al. (2003) modified this code to account for colloid attachment, detachment, straining, and size exclusion. HYDRUS-1D is coupled to a nonlinear least squares optimization routine to facilitate the determination of transport parameters from experimental data (effluent and/or deposition data). Aspects of HYDRUS-1D that are relevant to the manure suspension and/or *Giardia* transport experiments are briefly discussed below.

In the absence of death and/or inactivation processes, the aqueous phase manure suspension or *Giardia* mass balance equation is written as:

$$\frac{\partial(\theta_w C)}{\partial t} = -\nabla J_T - E_{sw} \quad [1]$$

where C is the concentration [N_c L_e^{-3}; L_e denotes length] of manure particles or *Giardia* in the aqueous phase, t [T] is time, θ_w [-] is the volumetric water content, J_T [N_c L_e^{-2} T^{-1}] is the total flux (sum of the advective, dispersive, and diffusive fluxes) of manure particles or *Giardia*, and E_{sw} [N_c L_e^{-3} T^{-1}] is the manure particle or *Giardia* mass transfer terms between the aqueous and solid phases.

Due to the complex physical and chemical nature of the manure suspension and the large size of cysts of *Giardia*, a simple and flexible 1-site kinetic model formulation for E_{sw} will be employed. This approach lumps straining and attachment deposition processes together and no attempt will be made to separately quantify these mechanisms. The value of E_{sw} is determined as follows:

$$E_{sw} = \frac{\partial(\rho_b S)}{\partial t} = \theta_w k_1 \psi_1 C \quad [2]$$

Here ρ_b [M L_e^{-3}; M denotes mass] is the soil bulk density, S [N_c M^{-1}] is the solid phase concentration of deposited manure particles or *Giardia* cysts, k_1 [T^{-1}] is the deposition rate coefficient, and ψ_1 [-] is a dimensionless deposition function. The value of ψ_1 is modeled as a function of distance and S as follows:

$$\psi_1 = \left(1 - \frac{S}{S^{max}}\right)\left(\frac{d_{50} + z}{d_{50}}\right)^{-\beta} \quad [3]$$

where z [L_e] is the depth from the column inlet, S^{max} [N_c M^{-1}] is the maximum solid phase concentration of deposited manure particles or *Giardia*, and β [-] is a parameter that controls the shape of the spatial distribution. Bradford et al. (2003) found that the value of $\beta = 0.432$ gave a good description of the spatial distribution of retained carboxyl latex colloids (0.45–3.2 μm) when significant straining occurred. Since the average size of *Giardia* and the manure particles were much larger than these latex colloids and other experimental conditions were comparable, the value of β was set equal to 0.432 for all simulations considered herein. The first term on the right hand side of Eq. [3] accounts for filling and accessibility of deposition sites in a manner similar to the Langmuirian blocking approach (e.g., Deshpande and Shonnard, 1999). The remaining term on the right hand side of Eq. [3] assumes that manure particles or *Giardia* deposition follows a power law spatial distribution.

RESULTS AND DISCUSSION

Manure Suspension

Figure 1a presents effluent concentration (breakthrough) curves for the manure suspension in the 710-, 360-, 240-, and 150-μm Ottawa sands. Here relative effluent concentrations (C/C_i; where C_i is the initial influent concentration of manure suspension or cysts of *Giardia*) were plotted as a function of column PVs. In the plateau region of the breakthrough (~1 to 7.5 PV), C/C_i increased with increasing sand size for a given PV. For a given sand, values of C/C_i also tended to continue to increase with increasing PV. The slope of the breakthrough curve over the 1 to 6 PV range was 0.027, 0.055, 0.072, and 0.035 for the 710-, 360-, 240-, and 150-μm sands, respectively. Hence, the rate of increasing concentration appeared to be greatest for the intermediate grain size sands (240- and 360-μm sand). This time-dependent breakthrough behavior has frequently been ascribed to blocking of favorable attachment sites (e.g., Camesano et al., 1999), but may also be attributed to filling of straining sites (Bradford et al., 2005).

Figure 1b presents corresponding spatial distribution data for the manure particles retained in the various sands. Here the normalized concentration (number, N_c,

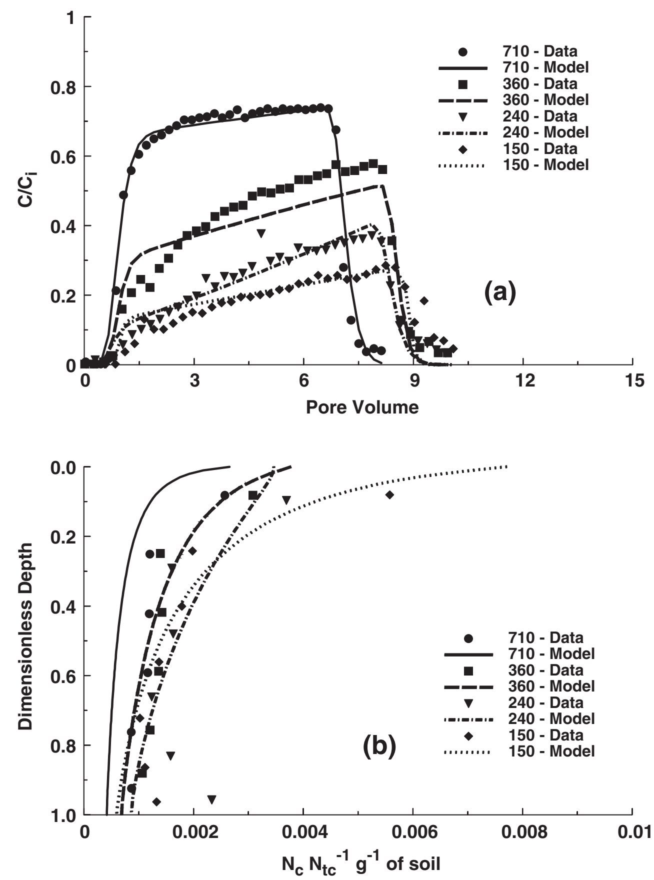

Fig. 1. (a) Observed and simulated effluent concentration curves and (b) spatial distributions for manure suspension in 710-, 360-, 240-, and 150-μm sand. Simulations considered deposition according to Eq. [1] to [3] and corresponding model parameters are given in Table 2.

Table 2. Model (Eq. [1]–[3]) and statistical parameters for simulated transport of the manure suspension.

Sand	λ_H	k_1	S^{*max}	β	r_e^2	r_s^2	MSE_e	MSE_s
μm	cm	h^{-1}	$N_c\ N_{ic}^{-1}\ g^{-1}$					
710	0.638	3.03	1.70	0.432	0.98	0.91	1.4×10^{-3}	1.3×10^{-1}
360	0.385	13.71	2.04	0.432	0.94	0.84	3.1×10^{-3}	3.1×10^{-2}
240	0.803	33.20	1.83	0.432	0.94	0.40	1.1×10^{-3}	1.5×10^{-1}
150	0.111	34.16	4.34	0.432	0.77	0.90	2.0×10^{-3}	9.1×10^{-2}

divided by the total number added to the column, N_{tc}) per gram of dry sand was plotted as a function of dimensionless depth (distance from the column inlet divided by the column length). The concentration near the inlet was highest and then rapidly decreased with increasing distance. Finer grained sands tended to produce greater deposition of manure particles, especially near the column inlet. Some scatter in the spatial distribution data also occurred, presumably due to changes in the manure suspension size distribution with passage through the sand. The manure effluent and spatial distribution data were generally consistent with straining behavior that was reported for latex microspheres (0.45–3.2 μm) in these same Ottawa sands by Bradford et al. (2002, 2003).

Figures 1a and 1b also present simulated transport of the manure suspension in the various sands. Table 2 provides a summary of fitted model parameters (dispersivity, λ_H; k_1; $S^{*max} = S^{max}/N_i$ where $N_i = C_i \times 1$ mL; and β), as well as statistical parameters to characterize the goodness of parameter fits. The coefficient of linear regression (Simunek and Hopmans, 2002) estimates the proportion of the variation to effluent (r_e^2) and spatial distribution (r_s^2) data that is explained by the model. The mean square error for effluent (MSE_e) and spatial distribution (MSE_s) data is used to quantify the magnitude of the deviation between observed and predicted quantities. Figures 1a and 1b and the statistical parameters in Table 2 indicate that the model generally provided a reasonable description of both effluent and spatial distribution data. Deviations in experimental data and simulations occurred in part due to the simultaneous fitting of effluent and spatial distribution data (see the effluent data for the 360-μm sand in Fig. 1a),

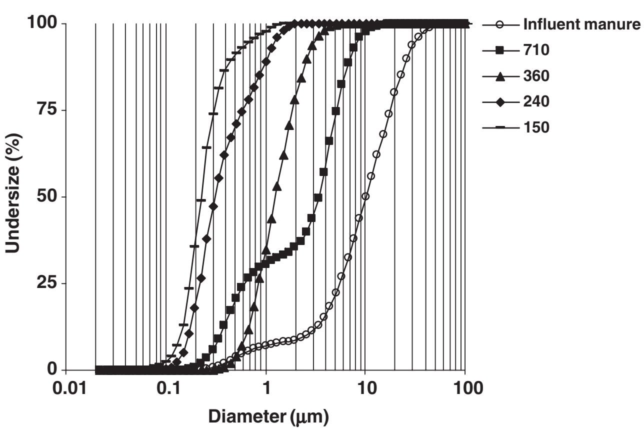

Fig. 2. The cumulative size distribution (CSD) for manure effluent in the 710-, 360-, 240-, and 150-μm sands after 95 min. The CSD of the influent manure suspension is also shown in the figure for reference.

and mass balance errors (see Table 1 and the spatial distribution data for the 710-μm sand in Fig. 1b). Lower values of r_s^2 and higher values of MSE_s in Table 2 were also associated with scatter in the spatial distribution data. An improved description of both effluent and spatial distribution data is possible if β is fitted (Bradford et al., 2003). A fixed value of $\beta = 0.432$ was chosen in these simulations to minimize the number of fitting parameters.

Inspection of Table 2 reveals trends in the fitted model parameters. The value of k_1 increased with decreasing sand size, indicating greater deposition (Fig. 1a and 1b). Values of S^{*max} tended to decrease with increasing sand size. This suggests that deposition sites are filled or blocked (time dependency of the breakthrough curves) more rapidly in the coarser-textured sand. A systematic relationship between λ_H and grain size was not found, possibly due to the confounding influence of sand uniformity/gradation or decreased sensitivity of simulation results to this parameter.

To elucidate the mechanisms controlling manure suspension transport and deposition, the particle-size distribution of the influent manure suspension and column effluents was periodically measured. Figure 2 presents the cumulative size distributions (CSDs) of manure particles in the effluent at 95 min (~2.5 PV) after passage through the various sands, as well as the CSD for the influent manure suspension. Manure particles larger than around 12, 5, 0.8, and 0.5 μm were completely removed after passage through the 710-, 360-, 240-, and 150-μm sands, respectively, due to mechanical filtration and/or straining. This corresponds to ratios of manure particle to median grain size of 0.003 to 0.017. These ratios are significantly smaller than the straining criterion of 0.18 proposed by Matthess and Pekdeger (1985), but are more consistent with the 0.005 guideline proposed by Bradford et al. (2003).

Additional measurements were conducted to examine temporal changes in the effluent CSD with continued addition of manure suspension. Figures 3a to 3d present the cumulative size distribution of effluent samples at various times (95–295 min; corresponding to 2.5–7.5 PV) in the 710-, 360-, 240-, and 150-μm sand, respectively. The CSDs indicate that the size of manure particles in the effluent samples was increasing with increasing time. Temporal changes in the effluent CSD, however, were highly sand-size specific. The greatest changes in the effluent CSD occurred at earlier times and for the finer-textured sands. These observations suggest that smaller pores that induced deposition by straining were becoming filled with manure particles. As these straining sites filled, water flow and manure particle transport was confined to the larger, more con-

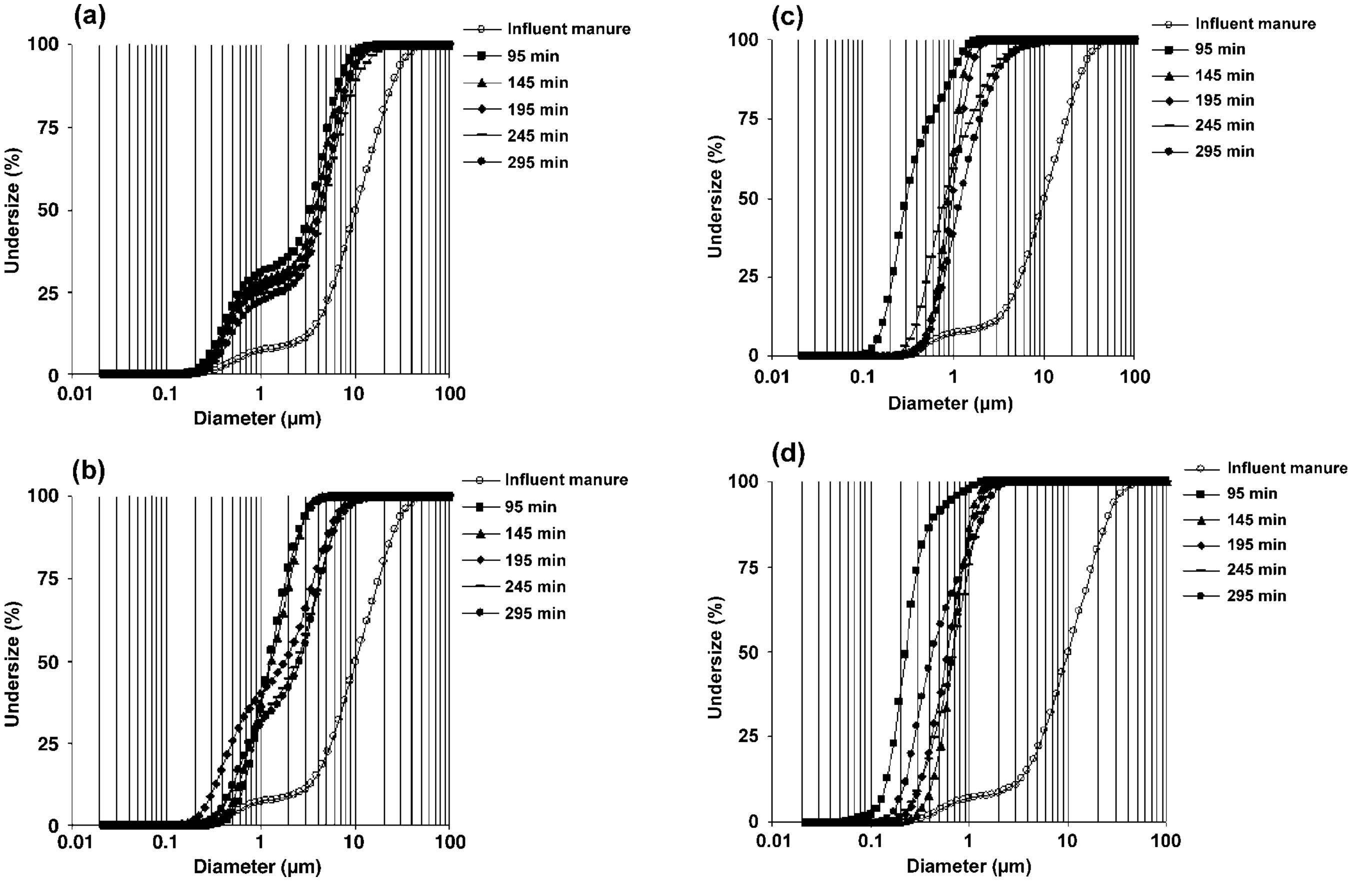

Fig. 3. The cumulative size distribution (CSD) for manure effluent in the (a) 710-μm, (b) 360-μm, (c) 240-μm, and (d) 150-μm sands after 95, 145, 195, 245, and 295 min. The CSD of the influent manure suspension is also shown in the figures for reference.

ductive pore spaces. Hence, temporal changes in the plateau regions of the effluent concentration curves shown in Fig. 1a were likely due to filling of straining sites. Temporal changes in the plateau region of colloid breakthrough curves have been typically attributed to blocking of favorable attachment sites (e.g., Camesano et al., 1999). This explanation cannot account for the observed temporal changes in the manure particle CSD shown Fig. 3a to 3d.

The CSD data shown in Fig. 2 and 3a to 3d have important implications for pathogen transport in these sands. First, Fig. 2 indicates that straining of pathogens is likely to occur for ratios of microbe diameter to median grain diameter greater than 0.003 to 0.017 (depending on the grain-size distribution characteristics). Second, Fig. 3a to 3d suggest that these straining sites will be filled over time as a result of deposition. This will diminish the deposition of larger sized pathogens with increasing time, and enhance their transport potential. Transport and deposition data for *Giardia* in the absence and presence of manure suspension will be discussed below, to provide illustrative examples of the roles of these straining processes.

Giardia Transport

Figures 4a and 4b present observed and simulated effluent concentration curves and spatial distributions for *Giardia* in the 710-, 360-, and 150-μm sands in the absence of manure suspension. In this case, very few *Giardia* were transported through the sands (the value of C/C_i on the y axis of Fig. 4a only goes from 0 to 0.12). Table 1 provides percentage recovery information for *Giardia* in the effluent and sand, as well as the total system. No *Giardia* were recovered in the effluent for the 150-μm sand, and only 1.8 and 0.4% were recovered in the effluent for the coarsest 710- and 360-μm sands, respectively. These low percentage recoveries were consistent with the effluent particle-size distribution information for manure particles that was presented in Fig. 2 and 3. Furthermore, the spatial distribution information for *Giardia* in Fig. 4b was also similar to that shown for the manure particles (Fig. 1b). All of these observations indicate that the deposition of *Giardia* was controlled by straining, which occurs primarily in the sand adjacent to the column inlet.

Figures 5a and 5b present observed and simulated effluent concentration curves and spatial distributions for *Giardia* in the 710-, 360-, and 150-μm sands when in the presence of manure suspension. Effluent and spatial distribution data for the cysts in the presence (Fig. 5a and 5b) and absence (Fig. 4a and 4b) of manure suspension exhibited many similarities. For example, effluent concentrations were low and tended to increase in magnitude with increasing sand size. The spatial distribution data indicate that retention occurred primarily

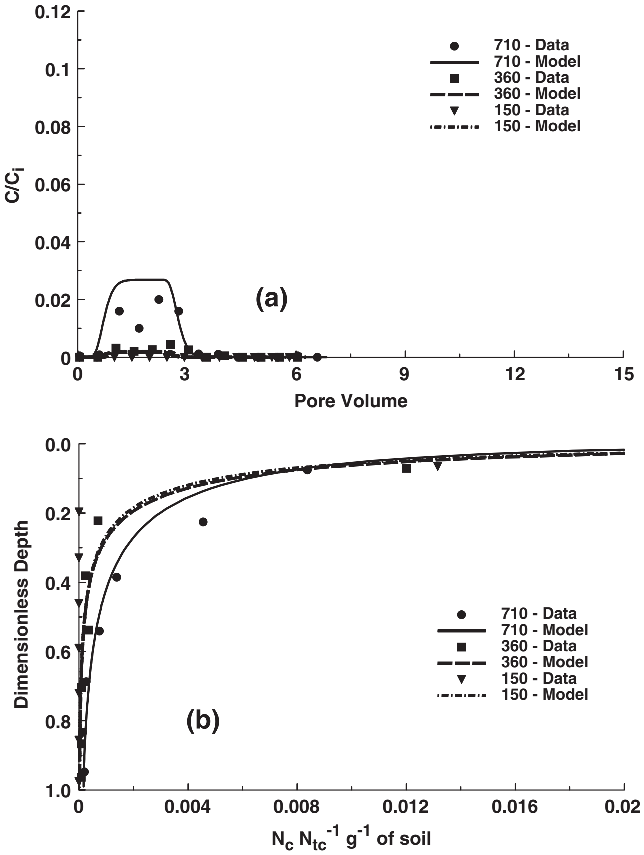

Fig. 4. (a) Observed and simulated effluent concentration curves and (b) spatial distributions for *Giardia* in the 710-, 360-, and 150-μm sands in the absence of manure suspension. Here simulations considered deposition according to Eq. [1] to [3] and corresponding model parameters are provided in Table 3.

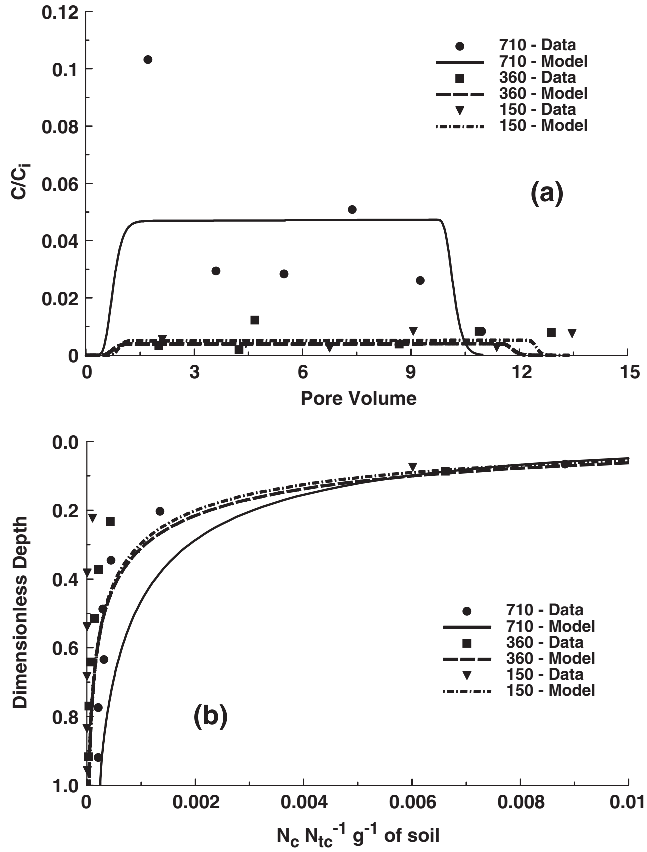

Fig. 5. (a) Observed and simulated effluent concentration curves and (b) spatial distributions for *Giardia* in the 710-, 360-, and 150-μm sands in the presence of manure suspension. Here simulations considered deposition according to Eq. [1] to [3] and corresponding model parameters are provided in Table 3.

near the column inlet and increased with decreasing sand size. In contrast to Fig. 4a and 4b (absence of manure suspension), cyst transport in the presence of manure suspension produced slightly higher effluent concentrations and greater deposition behavior near the column inlet in the coarser textured sand (710 μm). For a given sand the difference in F_{eff} for *Giardia* in the presence and absence of manure was 0.3 to 3.1% (Table 1), with greater differences occurring in coarser-textured sands. Although these increases were low, the relative increase was very high (75 and 172% increase for the 360- and 710-μm sands, respectively). An explanation for this increase in the presence of manure can be obtained from the CSD for manure effluent shown in Fig. 3a to 3d. Recall that larger manure particles were transported through the sands as the amount of manure added to the column increased. This was interpreted as a result of filling or blocking of straining sites.

The simulations shown in Fig. 4a, 4b, 5a, and 5b indicate that the model gave a reasonable description of the *Giardia* transport data in the presence and absence of manure suspension. Table 3 provides a summary of model parameters, as well as statistical parameters to characterize the goodness of parameter fits. The low values of $\mathrm{MSE_e}$ in Table 3 indicate that little deviation occurred between observed and simulated effluent data. The r_s^2 values were also quite high (>0.95) and the simulations therefore provided a good characterization

Table 3. Model (Eq. [1]–[3]) and statistical parameters for simulated transport of the *Giardia* in the presence and absence of manure suspension. Values of λ_H were obtained from Table 2 for the manure suspension, and $S^{*\max}$ was set equal to 1000 to minimize the dependence of ψ_1 on S in Eq. [3].

Sand	λ_H	k_1	$S^{*\max}$	β	r_e^2	r_s^2	$\mathrm{MSE_e}$	$\mathrm{MSE_s}$
μm	cm	$\mathrm{h^{-1}}$	$N_c\,N_{ic}^{-1}\,\mathrm{g^{-1}}$					
710	0.638	39.54	1000.0	0.432	0.80	0.95	3.6×10^{-5}	1.6×10^{-2}
360	0.385	84.56	1000.0	0.432	0.55	0.98	1.6×10^{-6}	3.3×10^{-2}
150	0.111	101.40	1000.0	0.432	0.00	0.96	1.1×10^{-6}	6.2×10^{-2}
710†	0.638	22.90	1000.0	0.432	0.23	0.95	7.3×10^{-4}	4.9×10^{-1}
360†	0.385	64.27	1000.0	0.432	0.04	0.97	2.6×10^{-5}	2.2×10^{-1}
150†	0.111	82.20	1000.0	0.432	0.24	0.96	1.4×10^{-5}	6.5×10^{-1}

† Experiments conducted in the presence of manure suspension (4 g $\mathrm{L^{-1}}$).

of the observed deposition profiles. For a given sand, values of k_1 were lower in the presence than in the absence of manure suspension, suggesting that manure particles filled straining sites and decreased deposition. For a given solution composition (presence or absence of manure), the value of k_1 increased with decreasing sand size due to greater deposition. Values of F_{total} were also found to decrease with decreasing sand size. This likely occurred as a result of increasing deposition near the column inlet (Fig. 4b). Accurate measurements of *Giardia* mass balance are believed to be more difficult when the vast majority of the cysts were concentrated in a single measurement point (very high counts) in the sand near the column inlet; especially when manure particles were also present in high concentrations.

CONCLUSIONS

Mechanisms of manure suspension transport and deposition were studied in saturated column experiments. The peak effluent concentration decreased and the deposition in the sand near the column inlet increased with a decrease in sand grain size. Mechanisms that were controlling the manure particle deposition were identified by measuring the cumulative size distribution of manure components in the suspension initially and after passage through the packed columns. The CSD data indicated that manure particles were completely removed at early times by straining when d_p/d_{50} (d_p = manure particle diameter) was greater than 0.003 to 0.017. However, as time progressed the effluent CSD tended to become closer to the influent manure CSD due to deposition induced filling of these straining sites. This produced increasing effluent concentrations and transport of larger sized manure particles with increasing time. Simulations of the manure transport using a simple and flexible power law model for the solid-water mass exchange term provided a satisfactory description of the effluent and spatial distribution data for the manure suspension.

The observed transport and deposition behavior for manure particles has important implications for manure-borne pathogen transport. For the considered experimental conditions, straining of pathogens was likely to occur for values of $d_p/d_{50} > 0.003$. Furthermore, straining sites were likely to be filled over time as a result of deposition. This last observation indicates that deposition of larger sized pathogens may decrease with time, thus enhancing their transport potential. To further investigate these findings, transport and deposition experiments for cysts of *Giardia* in the absence and presence of manure suspensions were conducted. In the absence of manure suspension, *Giardia* had low transport potential and deposition was controlled by straining. For a given sand, higher effluent concentrations of *Giardia* occurred in the presence than in the absence of manure suspension due to filling of straining sites by manure particles. Hence, pathogen transport studies conducted in the absence of manure suspension may underestimate transport potential in manure-contaminated environments.

ACKNOWLEDGMENTS

This research was supported by the 206 Manure and By-product Utilization Program of the USDA–ARS. Mention of trade names and company names in this manuscript does not imply any endorsement or preferential treatment by the USDA.

REFERENCES

Bales, R.C., S. Li, K.M. Maguire, M.T. Yahya, and C.P. Gerba. 1993. MS-2 and poliovirus transport in porous media: Hydrophobic effects and chemical perturbations. Water Resour. Res. 29:957–963.

Bradford, S.A., and L.M. Abriola. 2001. Dissolution of residual tetrachloroethylene in fractional wettability porous media: Incorporation of interfacial area estimates. Water Resour. Res. 37:1183–1195.

Bradford, S.A., and M. Bettahar. 2005. Straining, attachment, and detachment, of *Cryptosporidium* oocysts in saturated porous media. J. Environ. Qual. 34:469–478.

Bradford, S.A., M. Bettahar, J. Simunek, and M.Th. van Genuchten. 2004. Straining and attachment of colloids in physically heterogeneous porous media. Vadose Zone J. 3:384–394.

Bradford, S.A., and J. Schijven. 2002. Release of *Cryptosporidium* and *Giardia* from dairy calf manure: Impact of solution salinity. Environ. Sci. Technol. 36:3916–3923.

Bradford, S.A., J. Simunek, M. Bettahar, Y.F. Tadassa, M.Th. van Genuchten, and S.R. Yates. 2005. Straining of colloids at textural interfaces. Water Resour. Res. 41:W10404, doi:10.1029/2004WR003675.

Bradford, S.A., J. Simunek, M. Bettahar, M.Th. van Genuchten, and S.R. Yates. 2003. Modeling colloid attachment, straining, and exclusion in saturated porous media. Environ. Sci. Technol. 37:2242–2250.

Bradford, S.A., S.R. Yates, M. Bettahar, and J. Simunek. 2002. Physical factors affecting the transport and fate of colloids in saturated porous media. Water Resour. Res. 38(12):1327, doi:10.1029/2002WR001340.

Brush, C.F., W.C. Ghiorse, L.J. Anguish, J.-Y. Parlange, and H.G. Grimes. 1999. Transport of *Cryptosporidium parvum* oocysts through saturated columns. J. Environ. Qual. 28:809–815.

Camesano, T.A., K.M. Unice, and B.E. Logan. 1999. Blocking and ripening of colloids in porous media and their implications for bacterial transport. Colloids Surf. A 160:291–308.

Danielson, R.E., and P.L. Sutherland. 1986. Porosity. *In* A. Klute (ed.) Methods of soil analysis. Part 1. 2nd ed. SSSA, Madison, WI.

de Jonge, L.W., C. Kjaergaard, and P. Moldrup. 2004. Colloids and colloid-facilitated transport of contaminants in soils: An introduction. Vadose Zone J. 3:321–325.

Deshpande, P.A., and D.R. Shonnard. 1999. Modeling the effects of systematic variation in ionic strength on the attachment kinetics of Pseudomonas fluorescens UPER-1 in saturated sand columns. Water Resour. Res. 35:1619–1627.

Elimelech, M., and C.R. O'Melia. 1990. Kinetics of deposition of colloidal particles in porous media. Environ. Sci. Technol. 24: 1528–1536.

Foppen, J.W.A., A. Mporokoso, and J.F. Schijven. 2005. Determining straining of *Escherichia coli* from breakthrough curves. J. Contam. Hydrol. 76:191–210.

Gerba, C.P., J.B. Rose, and C.N. Haas. 1996. Sensitive populations: Who is at the greatest risk? Int. J. Food. Microbiol. 30:113–123.

Gerritson, J., and S.W. Bradley. 1987. Electrophoretic mobility of natural particles and cultured organisms in freshwaters. Limnol. Oceanogr. 32:1049–1058.

Ginn, T.R., B.D. Wood, K.E. Nelson, T.D. Schiebe, E.M. Murphy, and T.P. Clement. 2002. Processes in microbial transport in the natural subsurface. Adv. Water Res. 25:1017–1042.

Hancock, C.M., J.B. Rose, and M. Callahan. 1998. *Crypto* and *Giardia* in US ground water. J. Am. Water Works Assoc. 90:58–61.

Harter, T., S. Wagner, and E.R. Atwill. 2000. Colloid transport and filtration of *Cryptosporidium parvum* in sandy soils and aquifer sediments. Environ. Sci. Technol. 34:62–70.

Harvey, R.W., and H. Harms. 2002. Transport of microorganisms in the terrestrial subsurface: In situ and laboratory methods. p. 753–776. *In* C. Hurst et al. (ed.) Manual of environmental microbiology. 2nd ed. ASM Press, Washington, DC.

Herzig, J.P., D.M. Leclerc, and P. LeGoff. 1970. Flow of suspension through porous media: Application to deep filtration. Ind. Eng. Chem. 62:129–157.

Hoogenboezem, W., H.A.M. Ketelaars, G.J. Medema, G.B.J. Rijs, and J.F. Schijven. 2001. *Cryptosporidium* and *Giardia*: Occurrence in sewage, manure and surface water. RIWA/RIVM/RIZA, Bilthoven, the Netherlands.

Hsu, B.-M., C. Huang, and J.R. Pan. 2001. Filtration behaviors of Giardia and Cryptosporidium: Ionic strength and pH effects. Water Res. 16:3777–3782.

Jin, Y., Y. Chu, and Y. Li. 2000. Virus removal and transport in saturated and unsaturated sand columns. J. Contam. Hydrol. 43:111–128.

Jin, Y., and M. Flury. 2002. Fate and transport of viruses in porous media. Adv. Agron. 77:39–102.

Johnson, W.P., and B.E. Logan. 1996. Enhanced transport of bacteria in porous media by sediment-phase and aqueous-phase natural organic matter. Water Res. 30:923–931.

Kellogg, R.L., C.H. Lander, D.C. Moffitt, and N. Gollehon. 2000. Manure nutrients relative to the capacity of cropland and pastureland to assimilate nutrients—spatial and temporal trends for the United States. GSA Publ. nsp00-0579. USDA Natural Resources Conserv. Service and Economic Res. Service, Riverside, CA.

Kinoshita, T., R.C. Bales, K.M. Maguire, and C.P. Greba. 1993. Effect of pH on bacteriophage transport through sandy soils. J. Contam. Hydrol. 14:55–70.

Logan, A.J., T.K. Stevik, R.L. Siegrist, and R.M. Ronn. 2001. Transport and fate of *Cryptosporidium parvum* oocysts in intermittent sand filters. Water Res. 35:4359–4369.

Loge, F.J., D.E. Thompson, and R.C. Douglas. 2002. PCR detection of specific pathogens in water: A risk-based analysis. Environ. Sci. Technol. 36:2754–2759.

Matthess, G., and A. Pekdeger. 1985. Survival and transport of pathogenic bacteria and viruses in groundwater. p. 472–482. *In* C.H. Ward et al. (ed.) Ground water quality. John Wiley & Sons, New York.

Mawdsley, J.L., A.E. Brooks, and R.J. Merry. 1996a. Movement of the protozoan pathogen *Cryptosporidium parvum* through three contrasting soil types. Biol. Fertil. Soils 21:30–36.

Mawdsley, J.L., A.E. Brooks, R.J. Meryy, and B.F. Pain. 1996b. Use of a novel soil tilting table apparatus to demonstrate the horizontal and vertical movement of the protozoan pathogen *Cryptosporidium parvum* in soil. Biol. Fertil. Soils 23:215–220.

McDowell-Boyer, L.M., J.R. Hunt, and N. Sitar. 1986. Particle transport through porous media. Water Resour. Res. 22:1901–1921.

Medema, G.J., F.M. Schets, P.F.M. Teunis, and A.H. Havelaar. 1998. Sedimentation of free and attached *Cryptosporidium* oocysts and *Giardia* cysts in water. Appl. Environ. Microbiol. 64:4460–4466.

Pieper, A.P., J.N. Ryan, R.W. Harvey, G.L. Amy, T.H. Illangasekare, and D.W. Metge. 1997. Transport and recovery of bacteriophage PRD1 in a sand and gravel aquifer: Effect of sewage-derived organic matter. Environ. Sci. Technol. 31:1163–1170.

Powelson, D.K., and A.L. Mills. 2001. Transport of Escherichia coli in sand columns with constant and changing water contents. J. Environ. Qual. 30:238–245.

Schijven, J.K., and S.M. Hassanizadeh. 2000. Removal of viruses by soil passage: Overview of modeling, processes, and parameters. Crit. Rev. Environ. Sci. Technol. 30:49–127.

Sharma, M.M., Y.I. Chang, and T.F. Yen. 1985. Reversible and irreversible surface charge modification of bacteria for facilitating transport through porous media. Colloids Surf. 16:193–206.

Simunek, J., and J.W. Hopmans. 2002. Parameter optimization and nonlinear fitting. p. 139–157. *In* J.H. Dane and G.C. Topp (ed.) Methods of soil analysis. Part 4. SSSA Book Ser. 5. SSSA, Madison, WI.

Simunek, J., K. Huang, M. Sejna, and M.Th. van Genuchten. 1998. The HYDRUS-1D software package for simulating the one-dimensional movement of water, heat, and multiple solutes in variably-saturated media. Version 2.0. IGWMC-TPS-70. International Ground Water Modeling Ctr., Colorado School of Mines, Golden, CO.

Swertfeger, J., D.H. Metz, J. DeMarco, A. Braghetta, and J.B. Jacangelo. 1999. Effect of filter media on cyst and oocyst removal. J. Am. Water Works Assoc. 91:90–100.

Tufenkji, N., and M. Elimelech. 2005. Spatial distributions of Crypotsporidium oocysts in porous media: Evidence for dual model deposition. Environ. Sci. Technol. 39:3620–3629.

Tufenkji, N., G.F. Miller, J.N. Ryan, R.W. Harvey, and M. Elimelech. 2004. Transport of *Cryptosporidium* oocysts in porous media: Role of straining and physicochemical filtration. Environ. Sci. Technol. 38:5932–5938.

Tufenkji, N., J.A. Redman, and M. Elimelech. 2003. Interpreting deposition patterns of microbial particles in laboratory-scale column experiments. Environ. Sci. Technol. 37:616–623.

USEPA. 2000. National primary drinking water regulations: Ground water rule, proposed rule. Fed. Regist. 10:30194–30274.

van Genuchten, M.Th., F.J. Leij, and S.R. Yates. 1991. The RETC code for quantifying the hydraulic functions of unsaturated soils. USEPA Rep. 600/2-91/065. USEPA, Washington, DC.